Laboratori Nazionali di Frascati

LNF-61/61 (1961)

# G. Da Prato: SINGLE PION PRODUCTION IN PROTON-PROTON COLLISIONS ACCORDING TO THE ONE-PARTICLE EXCHANGE MODEL.

Estratto dal: Nuovo Cimento, 22, 123 (1961)

IL NUOVO CIMENTO Vol. XXII, N. 1 1° Ottobre 1961

# Single Pion Production in Proton-Proton Collisions According to the One-Particle Exchange Model.

G. Da Prato

*Laboratori Nazionali del C.N.E.N. - Frascati*

(ricevuto il 16 Luglio 1961)

**Summary.** — Single pion production in nucleon-nucleon collisions is calculated in the one-pion exchange approximation. All the possible diagrams of this kind are calculated in the « pole » approximation discussed in the text: also the interferences between them are taken into account. The lab. energy spectra of the final nucleons are calculated and compared with the experimental data at 2.85 GeV. This comparison shows a remarkably good agreement for small values of the squared 4-momentum of the virtual pion. For higher values the qualitative behaviour is still reproduced, but the theoretical absolute values are larger than the experimental ones.

## 1. – Introduction.

We want to study the processes of single pion production in proton-proton collisions, namely the reactions:

$$p+p \to p+n+\pi^+ \tag{1}$$

$$p+p \to p+p+\pi^0 \tag{2}$$

by using the model which describes the processes as occurring through the exchange of a single pion (Fig. 1).

This approach has been suggested by the fact that, in the last years, experimental evidence has been produced that in high energy inelastic processes small momentum transfers of the recoiling target particle are strongly favoured (1).

(1) J. G. Rushbrooke and D. Radojicic: *Phys. Rev. Lett.*, 5, 567 (1950); A. P. Batson, B. B. Culwick, J. G. Hill and L. Riddiford: *Proc. Roy. Soc. (London)*, 251, 218 (1959).

This situation can be qualitatively explained through a mechanism of interaction due to the exchange of a single pion (2), and for some particular reactions detailed calculations have been performed (3). The situation, however, is not yet completely clear, because in the quoted papers (3) drastic simplifications have been made, *e.g.* by neglecting some of the possible one-pion exchange (OPE) diagrams and the various mutual interference terms. New detailed experimental data on single pion production in proton-proton collision have recently been obtained at 2.85 GeV of the incident proton in the lab. system (4).

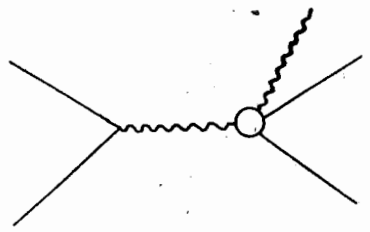

Fig. 1. – OPE diagram for the description of process (1) or (2). Full lines represent nucleons, dashed lines represent pions.

In the laboratory energy spectra of the final nucleons one finds again strong peaks corresponding to very small momentum transfers. This indicates again that the one-particle exchange plays an important role in the particular processes (1) and (2). We think it useful to calculate the spectra predicted by this model in the whole physical region by taking into account all the possible OPE effects. By comparing the prediction of the model with the experiment, we expect to find a sensibly good agreement in the region of small momentum transfers, where the further approximations made in order to obtain quantitative numerical results (5) can be well justified. These approximations consist in neglecting the influence of the « pion form factors » of the upper vertex in Fig. 1 and of the propagator of the virtual pion; and in considering as $\Delta^2$-independent (6) the partial wave amplitudes for the « off shell » pion-nucleon scattering. (The scattering angle which enters in the description of the lower vertex (5) is not taken on shell, but its dependence on $\Delta^2$ is taken into account.) For the region of higher momentum

(2) See for instance: F. SALZMAN and G. SALZMAN: *Phys. Rev.*, **120**, 599 (1960).

(3) E. FERRARI: *Nuovo Cimento*, **15**, 652 (1960) and *Phys. Rev.*, **120**, 988 (1960); S. D. DRELL: *Phys. Rev. Lett.*, **5**, 278, 342 (1960); F. SALZMAN and G. SALZMAN: *Phys. Rev. Lett.*, **5**, 377 (1960); J. IIZUKA and A. KLEIN: *Phys. Rev.* **123**, 669 (1961); F. SELLERI: *Phys. Rev. Lett.*, **6**, 64 (1961). In the last two papers an error of normali zation is contained. In both cases the theoretical predictions would be correct if multiplied by two.

(4) G. A. SMITH, H. COURANT, E. C. FOWLER, H. KRAYBILL, J. SANDWEISS and H. TAFT: Yale University, preprint. The experimental lab. energy spectra used in this paper are a private communication of the above authors. We thank Dr. G. A. SMITH and Prof. H. TAFT for having sent us these data.

(5) E. FERRARI and F. SELLERI: *Peripheral model for inelastic processes* (to be published as internal CERN report).

(6) Here we denote by $\Delta^2$ the square of the 4-momentum of the intermediate particle. We use the metric $p^2 = |\boldsymbol{p}|^2 - p_0^2$:

transfers we know a priori that these approximations are not good, but the comparison of the theory with the experiment can always give us a suggestion for approaching the problem of the OPE contribution when the intermediate particle is very virtual. We expect in this region to obtain an overestimate of the OPE contribution, which in all probability is mainly due to the neglected effects of the « pionic form factor » in the upper vertex of Fig. 1. Also the calculation of the interference effects generally involves at least one of the interfering terms considerably off shell. In this paper, however, it will be seen that these effects are not so important, and, in some cases, they turn out to be negligible.

Section 2 will be dedicated to notations and kinematics, Section 3 to the study of the lower vertex, Section 4 to the calculation of the differential cross-sections and finally Section 5 to the discussion of the obtained results.

## 2. – Notations, kinematics, Feynman graphs.

We denote by $p_1, k_1, p_2, k_2, q_2$ the energy-momentum 4-vectors of the incoming proton, target proton, outgoing proton, outgoing neutron (proton) for the first (second) reaction and outgoing pion respectively. We call $\mu$ the pion mass and $M$ the nucleon mass. Furthermore, we define the kinematical invariants

$$(3) \qquad W^2 = -(p_1 + k_1)^2, \qquad l^2 = -(k_2 + q_2)^2, \qquad u^2 = -(p_2 + q_2)^2,$$

$$\Delta^2 = (k_2 - k_1)^2, \qquad r^2 = (k_2 - p_1)^2, \qquad s^2 = (p_2 - k_1)^2, \qquad t^2 = (p_2 - p_1)^2$$

Among them the following relations hold

$$(4) \qquad \Delta^2 + r^2 + u^2 = s^2 + t^2 + l^2 = W^2 - 3M^2$$

$W$, $l$, $u$, are respectively: the total c.m. energy, the energy of $k_2$ and $q_2$ in their c.m. system and the energy of $p_2$ and $q_2$ in their c.m. system. $\Delta^2$, $r^2$, $s^2$, $t^2$ are nucleon momentum transfers.

Five of the invariants (3) are sufficient to obtain a complete description of the kinematics.

We will use also the following quantities:

*a*) In the c.m. system of $p_2$ and $q_2$ $\chi'$ is the 3-momentum of $p_2$ and $q_2$, $p'_{10}$, $k'_{10}$, $p'_{20}$, $k'_{20}$, $q'_{20}$ are the energies of $p_1$, $k_1$, $p_2$, $k_2$, $q_2$ respectively, $\varepsilon'$ is the angle between $p_2$ and $p_1$, $\beta'$ the angle between $p_2$ and $k_1$, $\alpha'$ the angle between $p_1$ and $k_1$, $\varphi'$ is the $p_2$ azimuthal angle in a frame of reference with the $z$ axis directed along $p_1$.

*b*) In the c.m. system of $p_2$ and $k_2$ the same quantities will be denoted by $\chi''$, $p''_{10}$, $k''_{10}$, $p''_{20}$, $k''_{20}$, $q''_{20}$, $\varepsilon''$, $\beta''$, $\alpha''$, $\varphi''$ respectively. Finally $T_L(p_2)$ and $T_L(k_2)$ will be the lab. kinetic energies of particles $p_2$ and $k_2$ respectively and $K$ the 3-momentum of $p_1$ and $k_1$ in the c.m. system. We have

$$T_L(k_2) = \frac{\Delta^2}{2M}, \qquad T_L(p_2) = \frac{s^2}{2M}. \tag{5}$$

The expression of the other kinematical quantities as functions of the invariants are given in [5].

The $T$ matrix is defined by

$$S_{fi} = \delta_{fi} + \frac{iM^2\delta^4(p_2 + k_2 + q_2 - p_1 - k_1)}{\sqrt{2}(2\pi)^{\frac{7}{2}}(p_{10}k_{10}p_{20}k_{20}q_{20})^{\frac{1}{2}}} T_{fi}, \tag{6}$$

$p_{10}$, $k_{10}$, $p_{20}$, $k_{20}$, $q_{20}$ are the energies in an arbitrary frame of reference. The differential cross-section $\mathrm{d}\sigma$ is given by

$$\mathrm{d}\sigma = \frac{M^4}{2(2\pi)^5 KW} \overline{\sum_{\text{spin}}} |T_{fi}|^2 \delta^4(p_2 + k_2 + q_2 - p_1 - k_1) \frac{\mathrm{d}^3p_2\, \mathrm{d}^3k_2\, \mathrm{d}^3q_2}{p_{20}k_{20}q_{20}}. \tag{7}$$

The bar over the summation symbol indicates the average over initial spins. Formula (7) is equivalent to:

$$\mathrm{d}\sigma = \frac{M^4}{8(2\pi)^4 K^2W^2} \overline{\sum_{\text{spin}}} |T_{fi}|^2 \frac{\chi'}{u} \mathrm{d}\cos\varepsilon'\, \mathrm{d}\varphi'\, \mathrm{d}u^2\, \mathrm{d}\Delta^2, \tag{8}$$

and also equivalent to

$$\mathrm{d}\sigma = \frac{M^4}{8(2\pi)^4 K^2W^2} \overline{\sum_{\text{spin}}} |T_{fi}|^2 \frac{\chi''}{l} \mathrm{d}\cos\varepsilon''\, \mathrm{d}\varphi''\, \mathrm{d}l^2\, \mathrm{d}s^2. \tag{9}$$

We shall use (8) for the $k_2$ particle spectrum and (9) for the $p_2$ particle spectrum.

The allowed physical region is determined from the following relations

$$0 \leqslant \varphi' \leqslant 2\pi \tag{10}$$

$$0 \leqslant \varepsilon' \leqslant \pi \tag{11}$$

$$(M+\mu)^2 \leqslant u^2 \leqslant \{M^2 + (W^2/2M^2)[2K(\Delta^4 + 4M^2\Delta^2)^{\frac{1}{2}} - \Delta^2 W]\} \tag{12}$$

$$\begin{cases} \frac{1}{2}\{W^2 - \mu^2 - 2M\mu - 4M^2 - (K/W)[(W^2 - \mu^2 - 2M\mu)^2 - 4M^2W^2]^{\frac{1}{2}}\} \leqslant \Delta^2 \\ \leqslant \frac{1}{2}\{W^2 - \mu^2 - 2M\mu - 4M^2 + (K/W)[(W^2 - \mu^2 - 2M\mu)^2 - 4M^2W^2]^{\frac{1}{2}}\} \end{cases} \tag{13}$$

for the case (8), and by the relation which we obtain by exchanging $\varphi' \to \varphi''$, $\varepsilon' \to \varepsilon''$, $u^2 \to l^2$, $\Delta^2 \to s^2$ for the case (9).

The four possibile Feynman graphs are given in Fig. 2.

Let $T_i^u$ and $T_i^l$ be the $T$ matrix elements relative to upper and lower vertices of the $i$-th graph. We have [7]

$$(14)\quad T_{fi} = \left[ \frac{\langle T_1^u \rangle \langle T_1^l \rangle}{\Delta^2 + \mu^2} + \frac{\langle T_3^u \rangle \langle T_3^l \rangle}{s^2 + \mu^2} - \frac{\langle T_2^u \rangle \langle T_2^l \rangle}{r^2 + \mu^2} - \frac{\langle T_4^u \rangle \langle T_4^l \rangle}{t^2 + \mu^2} \right],$$

for reaction (1) and

$$(15)\quad T_{fi} = \left[ \frac{\langle T_1^u \rangle \langle T_1^l \rangle}{\Delta^2 + \mu^2} + \frac{\langle T_4^u \rangle \langle T_4^l \rangle}{t + \mu^2} - \frac{\langle T_2^u \rangle \langle T_2^l \rangle}{r^2 + \mu^2} - \frac{\langle T_3^u \rangle \langle T_3^l \rangle}{s^2 + \mu^2} \right],$$

for reaction (2). The minus signs are due to the Pauli principle.

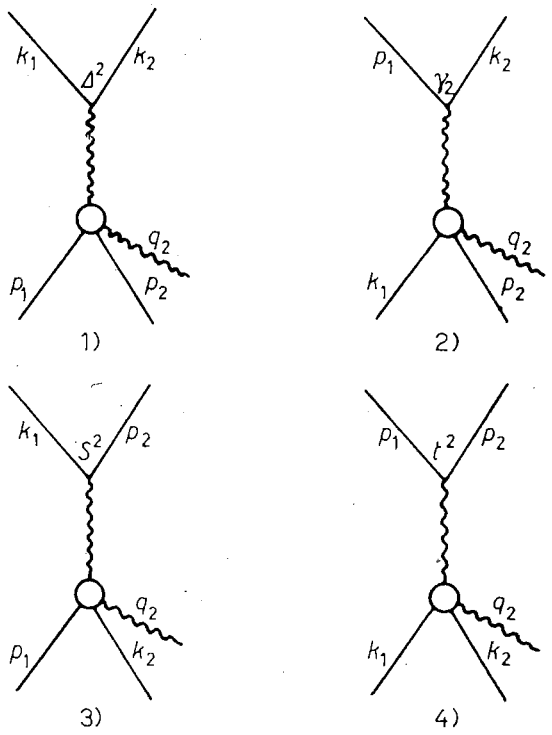


Fig. 2. – The possible OPE Feynman graphs for the process (1) or (2). In the upper vertices are written the relative momentum transfers.

## 3. – Pion-nucleon scattering amplitude.

Let $p_1$ and $p_2$ be the energy-momentum 4-vectors of the nucleons, and $q_1$ and $q_2$ those of the pions. We consider first the physical process; then $q_1^2 = -\mu^2$. The $T$ matrix elements are of the following form [8]

$$(16)\qquad \langle T^l \rangle = \bar{u}(p_2)(-A + iB\gamma \cdot q_2)u(p_1)$$

$u(p_2)$ and $u(p_1)$ are the nucleon spinors and $A$ and $B$ are given by

$$(17)\qquad \begin{cases} A = 4\pi \left( f_1 \dfrac{u + M}{p'_{20} + M} - f_2 \dfrac{u - M}{p'_{20} - M} \right), \\ B = 4\pi \left( f_1 \dfrac{1}{p'_{20} + M} + f_2 \dfrac{1}{p'_{20} - M} \right), \end{cases}$$

(7) Brackets stand for indices $fi$.

(8) G. F. CHEW, M. L. GOLDBERGER, F. E. LOW and Y. NAMBU: *Phys. Rev.*, **106**, 1337 (1957).

with

$$(18)\qquad \begin{cases} f_1 = \sum_{l=0}^{\infty} f_{l+} P'_{l+1}(\cos\varepsilon') - \sum_{l=2}^{\infty} f_{l-} P'_{l-1}(\cos\varepsilon') \\ f_2 = \sum_{l=1}^{\infty} (f_{l-} - f_{l+}) P'_l(\cos\varepsilon') , \end{cases}$$

$u$ is the total c.m. energy, $p'_{20}$ is the nucleon energy and $\varepsilon'$ the scattering angle in the c.m. system $P'_l$ are derivatives of Legendre polinomials. When $q_1$ goes off shell ($q_1^2 = \Delta^2$) formula (17) is modified in the following way [10]

$$(19)\qquad \begin{cases} A(u^2, \Delta^2) = 4\pi \left[ f_1(u^2, \Delta^2, t^2) \dfrac{u + M}{\sqrt{(p'_{10} + M)(p'_{20} + M)}} - \right. \\ \qquad\qquad \left. - f_2(u^2, \Delta^2, t^2) \dfrac{u - M}{\sqrt{(p'_{10} - M)(p'_{20} - M)}} \right], \\ B(u^2, \Delta^2) = 4\pi \left[ f_1(u^2, \Delta^2, t^2) \dfrac{1}{\sqrt{(p'_{10} + M)(p'_{20} + M)}} + \right. \\ \qquad\qquad \left. + f_2(u^2, \Delta^2, t^2) \dfrac{1}{\sqrt{(p'_{10} - M)(p'_{20} - M)}} \right]. \end{cases}$$

This definition leaves unchanged the bidimensional representation of the $T$ matrix elements [8] where the only $\Delta^2$-dependence is contained in $f_1$ and $f_2$ (*). In the expression (18) the whole $t^2$-dependence is contained in $\cos\varepsilon'$, which can be easily « extrapolated » off shell by means of its definition

$$(20)\qquad \cos\varepsilon' = \frac{2p'_{10}p'_{20} - 2M^2 - t^2}{2|\boldsymbol{p}'_1||\boldsymbol{p}'_2|} ,$$

while the amplitudes $f_{l\pm}$a re considered as $\Delta^2$-independent. This procedure can be trusted only at low $\Delta^2$: but it is at present the simplest one and gives the extension of CHEW and LOW's formula [9] to the whole physical region.

Quantities (19) will be used in the calculation of graph 1. In graphs 2, 3, 4. we have as arguments of $A$ and $B$ $u^2r^2$, $l^2s^2$, $l^2t^2$ respectively.

The reactions occurring in the lower vertex are:

$$(21)\qquad \pi^+ + \mathrm{p} \to \pi^+ + \mathrm{p}$$

$$(22)\qquad \pi^0 + \mathrm{p} \to \pi^+ + \mathrm{n}$$

(*) See also [5] for a discussion of this subject.

[9] G. F. CHEW and F. E. LOW: *Phys. Rev.*, **113**, 1640 (1959).

[10] In the following, we shall write $A(u^2, \Delta^2)$ instead of $(u^2, \Delta^2, t^2)$ and so on: the obvious momentum transfer-dependence is dropped for simplicity.

for reaction (1) and

$$\pi^0+\mathrm{p}\to\pi^0+\mathrm{p} \tag{23}$$

for reaction (2).

Reaction (21) is in a pure $\frac{3}{2}$ isotopic state and the only important wave is the $p^{\frac{3}{2}}$ wave. For this reason for the calculations of $\langle T^l\rangle$ relative to (21) we have considered only $f_{1+}$ different from 0; we use for it the one-resonance level formula [11]

$$\begin{cases} f_{1+}(u)=\dfrac{1}{2\chi'}\dfrac{\Gamma_1}{(u_1-u)-i(\Gamma_1/2)}\,, \\ \Gamma_1=\dfrac{2(\chi a)^3}{1+(\chi a)^2}\gamma_\lambda^2\,, \end{cases} \tag{24}$$

with $a=5.91$, $\gamma_\lambda^2=0.062\,5$, $u_1=1.314$ in units of proton mass [12]. Reaction (22) contains a mixture of $\frac{3}{2}$ and $\frac{1}{2}$ isotopic spin states. With increasing energy $p_{\frac{3}{2}}^{\frac{3}{2}}$, $d_{\frac{3}{2}}^{\frac{1}{2}}$, $f_{\frac{5}{2}}^{\frac{1}{2}}$ waves become, in turn, dominant. In this case we have considered different from 0 only

$$f_{1+}^{\frac{3}{2}} \quad \text{for} \quad u\leqslant 1.51 \tag{25}$$

$$f_{2-}^{\frac{1}{2}} \quad \text{for} \quad 1.51\leqslant u\leqslant 1.69 \tag{26}$$

$$f_{3-}^{\frac{1}{2}} \quad \text{for} \quad u\geqslant 1.69 \tag{27}$$

$f_{2-}$ and $f_{3-}$ have been calculated by empirical one-resonance level formulas (valid only in the above-mentioned intervals) from the latest experimental data [13]. We obtain

$$f_{2-}(u)=\frac{1}{2.288\chi'}\frac{\Gamma_2}{(u_2-u)-i\Gamma_2/2}\,, \tag{28}$$

$$\begin{cases} \Gamma_2=68.23u^3-315.30u^2+485.21u-248.47 \\ u_2=1.619\,, \end{cases} \tag{29}$$

$$f_{3-}(u)=\frac{1}{2\chi'}\frac{\Gamma_3}{(u_3-u)-i\Gamma_3/2}\,, \tag{30}$$

$$\begin{cases} \Gamma_3=-7.96u^3+48.33u^2-96.27u+63.27 \\ u_3=1.800\,. \end{cases} \tag{31}$$

---

[11] M. GELL-MANN and K. WATSON: *Ann. Rev. Nucl. Sci.*, **4**, 219 (1954).

[12] We will express in the following all numerical results in units of proton mass. unless otherwise stated.

[13] P. FALK-VAIRANT and G. VALLADAS: Centre d'Etudes Nucléaires de Saclay, rapport à la conférence de Rochester (1960).

Reaction (23) contains also a mixture of isotopic spin states. $p^{\frac{3}{2}}$ waves are dominant in interval (25), $d^{\frac{3}{2}}$ and $f^{\frac{5}{2}}$ waves in intervals (26) and (27), but in the latter cases the $p^{\frac{3}{2}}$ wave is not negligible with respect to $d^{\frac{3}{2}}$ and $f^{\frac{5}{2}}$ waves, because it enters multiplied by a factor of 4 (when squared). For this reason the calculations relative to reaction (2) are somewhat more complicated than those relative to reaction (1). In the next section we will first consider reaction (1) and on this basis we will obtain a good approximation for the calculations of reaction (2).

## 4. – Spin summations.

By substituting in (14) the $\langle T_i^u \rangle$ calculated with the usual Feynman rules and the $\langle T_i^l \rangle$ obtained from (16) and (20), and finally by averaging over initial and summing over final spins we obtain for the first reaction

$$(32)\qquad |T|^2 = F_1(u^2, l^2, \Delta^2, s^2) + F_1(u^2, l^2, r^2, t^2) + \tfrac{1}{9}F_1(l^2, u^2, s^2, \Delta^2) + \\ + \tfrac{1}{9}F_1(l^2, u^2, t^2, r^2) + F_2(u^2, l^2, \Delta^2, s^2) + \tfrac{1}{9}F_2(l^2, u^2, s^2, \Delta^2) + \\ + \tfrac{1}{3}F_3(u^2, l^2, \Delta^2, s^2) + \tfrac{1}{3}F_3(u^2, l^2, r^2, t^2)$$

with

$$(33)\qquad F_1(u^2, l^2, \Delta^2, s^2) = \\ = \frac{2g^2u^2(2\pi)^2}{M^4}\,\frac{\Delta^2}{(\Delta^2+\mu^2)^2}\,\mathrm{Re}[f_1f_1^* + f_1f_2^*\cos\varepsilon' + f_2f_1^*\cos\varepsilon' + f_2f_2^*],$$

$$(34)\qquad F_2(u^2, l^2, \Delta^2, s^2) = \frac{2(2\pi)^2 g^2}{M^4}\,\frac{u^2}{(\Delta^2+\mu^2)(r^2+\mu^2)}\,\mathrm{Re}\{[(p'_{10}-M)(k'_{10}-M)]^{\frac{1}{2}}\cdot \\ \cdot[f_1f_1^*\cos\alpha' + f_2f_2^* + f_1f_2^*\cos\varepsilon' + f_2f_1^*\cos\beta'](u+M) + [(p'_{10}+M)(k'_{10}+M)]^{\frac{1}{2}}\cdot \\ \cdot[f_2f_2^*\cos\alpha' + f_1f_1^* + f_2f_1^*\cos\varepsilon' + f_1f_2^*\cos\beta'](u-M)\},$$

$$(35)\qquad F_3(u^2, l^2, \Delta^2, s^2) = -\frac{g^2}{4M^4}\,\frac{1}{(\Delta^2+\mu^2)(s^2+\mu^2)}\,\mathrm{Re}\{L[AA^* - \mu^2BB^*] - \\ - N[MBA^* + MAB^* + 2BB^*]\chi'(|\boldsymbol{p}'_1|\cos\varepsilon' + p'_{10}q'_{20}) + P[BA^* - AB^*] + \\ + Q[2BA^*(\chi'|\boldsymbol{p}'_1|\cos\varepsilon' + p'_{10}q'_{10}) + MAA^* + \mu^2BB^*]\}.$$

Here the $f_i$ are functions of $u^2$ and $\Delta^2$; $f_i^*$ are functions of $u^2$ and $\Delta^2$ in (33), of $u^2$ and $r^2$ in (34), of $l^2$ and $s^2$ in (35). We have

$$(36)\qquad L = up'_{20}(|\boldsymbol{p}'_1||\boldsymbol{k}'_1|\cos\alpha' + p'_{10}k'_{10}) - u\chi'k'_{10}|\boldsymbol{p}'_1|\cos\varepsilon' - \chi'|\boldsymbol{k}'_1|\cos\beta'\cdot \\ \cdot(up'_{10} - M^2) + M^2(M^2 - up'_{10} - k'_{10}p'_{20})$$

$$N = \chi' |\boldsymbol{p}_1'| (uk_{10}' - M^2) + \chi' |\boldsymbol{k}_1'| \cos\beta' u(u - p_{10}') + M^2(\mu^2 - p_{10}' q_{20}') + \tfrac{1}{2}(\Delta^2 + 2M^2)(\chi'^2 + p_{20}' q_{20}') \tag{37}$$

$$P = M\{\chi' |\boldsymbol{p}_1'| \cos\varepsilon'[W^2 - 3M^2 + \mu^2 + uk_{10}' + 2p_{10}'(q_{20}' - p_{20}' - k_{10}')] + \chi' |\boldsymbol{k}_1'| \cos\beta'(up_{10}' - M^2) + |\boldsymbol{k}_1'| |\boldsymbol{p}_1'| \cos\alpha'(2k_{10}' - u)M - q_{20}' p_{10}' k_{10}'(k_{20}' - p_{10}' + k_{10}') + M^2 q_{20}'(p_{10}' - k_{10}') + p_{10}' q_{20}'(\mu^2 - p_{10}' p_{20}') + M^2(\chi'^2 + p_{20}' q_{20}')\} \tag{38}$$

$$Q = M\{|\boldsymbol{k}_1'| |\boldsymbol{p}_1'| \cos\alpha' - \chi' |p_1'| \cos\varepsilon' + k_{10}'(u - p_{10}') + p_{20}'(k_{20}' - k_{10}')\} \tag{39}$$

$g$ is the renormalized pion-nucleon coupling constant

$$g^2 = \frac{16\pi M^2 f^2}{\mu^2}, \tag{40}$$

$$f^2 = 0.08\,. \tag{41}$$

The $f_1$ terms come from square moduli of the single graphs, the $F_2$ terms from interferences between graphs which differ for the exchange of the initial nucleons, and the $F_3$ terms from interferences between graphs which differ for the exchange of the final nucleons. The interference terms between graphs which differ for the exchange of both initial and final nucleons vanish. The factors $\frac{1}{3}$ and $\frac{1}{9}$ are due to isotopic spin.

By putting (32) into (8) and (9) we get the spectra of outgoing nucleons. In case (8) the integrals of the first, the second and the fourth term can be easily reduced to single integrals because the integrands are $\varphi'$-independent (5). We can get a similar reduction also in case (9).

The main contributions to the cross-section are due to the $F_1$ terms. At 2.85 GeV, the $F_2$ terms give a contribution about five times as small as the $F_1$ terms the $F_3$ terms give a negligible contribution. We note also that the $F_2$ terms are the smaller the larger is the number of waves occurring.

Consider reaction (2). In this case we neglect the interference terms $F_3$, because they are the same as in the previous case, apart from isotopic spin factors. For the other terms we use formula (33) (without the $F_3$ terms) with the following additional modifications:

*a*) the numerical coefficient in front of all the $F_1$ and $F_2$ terms is $\frac{1}{18}$;

*b*) for $F_1$ terms we have assumed the following expressions in intervals (25), (26) and (27) for $f_1$ and $f_2$

$$\begin{cases} f_1 = 6f_{1+}\cos\varepsilon' \\ f_2 = -2f_{1+} \end{cases}, \tag{41'}$$

$$\begin{cases} f_1 = 6f_{1+}\cos\varepsilon' - f_{2-} \\ f_2 = -2f_{1+} + 3f_{2-}\cos\varepsilon' \end{cases} \tag{42}$$

and

$$(43) \qquad \begin{cases} f_1 = 6f_{1+}\cos\varepsilon' - 3f_{3-}\cos\varepsilon' \\ f_2 = -2f_{1+} + f_{3-}\tfrac{3}{2}(5\cos^2\varepsilon' - 1) \end{cases}$$

respectively.

## 5. – Concluding remarks.

Numerical results at 2.85 GeV for reactions (1) and (2) are shown and compared with experimental data in Figs. 3, 4 and 5. The agreement is very good when the squared four-momentum of the virtual pion is small (of the order of few times the squared π-meson mass). Not only the presence and the exact position of the low and high energy peaks are correctly predicted, but also their absolute normalization is reproduced within the experimental errors. This, to our opinion, definitely suggests that the one-pion exchange contribution plays an important role in the description of processes (1) and (2). Let us analyse the general behaviour of Figs. 3 and 4 referring to reaction (1).

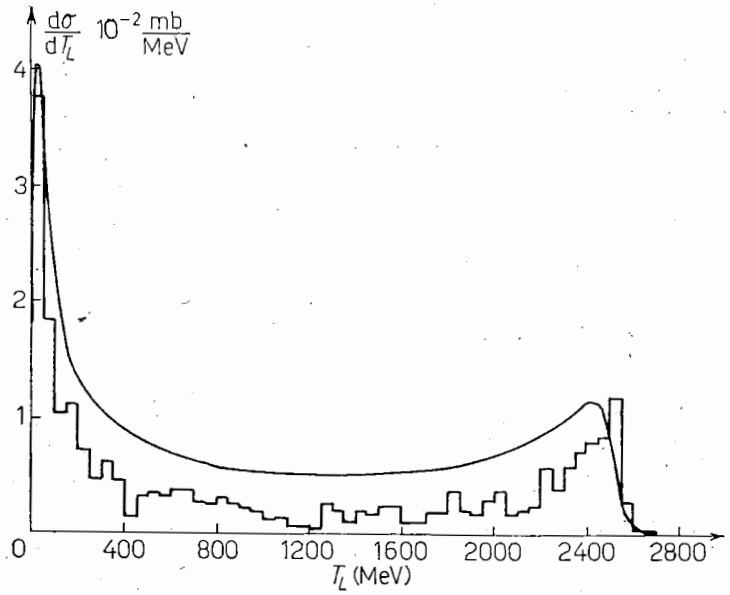


Fig. 3. – Theoretical and experimental spectrum of outgoing neutrons in the lab. system for the $p+p \to p+n+\pi^+$ reaction at 2.85 GeV of kinetic energy in the lab. system of the incoming protons.

As we said already in the text, all the interferences between the diagrams in Fig. 2 turn out to be small. Therefore, we can discuss, in a first approximation, the four diagrams separately. The largest contribution is always given from the graphs 1 and 2 of Fig. 2, where the $\pi^+$ comes out with the proton and allows the formation of the pure $T = J = \frac{3}{2}$ resonance. The squared matrix element of graph 1 contains the factor $\Delta^2(\Delta^2 + \mu^2)^{-2}$ which would give alone a steep maximum at $\Delta^2 \simeq \mu^2$. The further $\Delta^2$-dependence of the cross-section, given from the phase space limitations on the integration over the other dynamical variables, shifts this maximum to $\Delta^2 \simeq 2\mu^2$. Due to the proportionality of $\Delta^2$ to the lab. neutron energy, this gives the low

energy peak in Fig. 3. The high energy peak, which exists again for low values of the squared four-momentum of the virtual pion ($r^2$ this time), is contributed from graph 2. Its existence can be understood as follows. Graph 1 gives a strong backward peak of the neutrons in the c.m. angular distribution. Graph 2 gives a symmetric c.m. forward peak. The fact that these diagrams give a symmetric contribution is simply an effect of the Pauli principle, stating that all the final particles in a reaction in which the initial ones are identical, must have a c.m. angular distribution symmetric around 90°. The forward neutrons in the c.m. will then give rise to the high energy peak in the lab. system, while the backward ones give rise to the low energy peak. This effect is enhanced by the presence of the 33 resonance in the lower vertices. For the proton spectrum the argument is similar, though a little more complicated. The protons from graphs 1 and 2 are coming out together with a $\pi^+$. Tendency of formation of the 33 isobar will be shown. It should be clear that since the c.m. angular distribution of the « isobar » is the same as that of the neutron and since the proton is much heavier than the pion (the kinetic relative energy being small), its angular distribution will again be peaked forward and backward, though less markedly than for the neutron. Therefore, again, we should expect high and low energy peaks in the proton lab. spectra, of course broader than in the neutron case. Practically for the high energy peak the

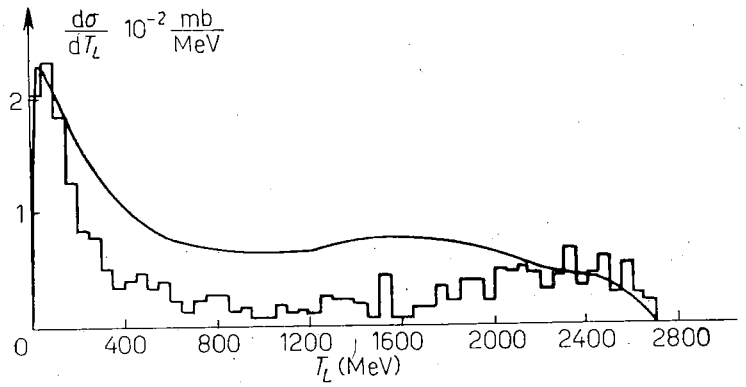


Fig. 4. – Theoretical and experimental spectrum of outgoing protons in the lab. system for the reaction $p+p \to p+n+\pi^+$ at 2.85 GeV of kinetic energy in the lab. system of the incoming protons.

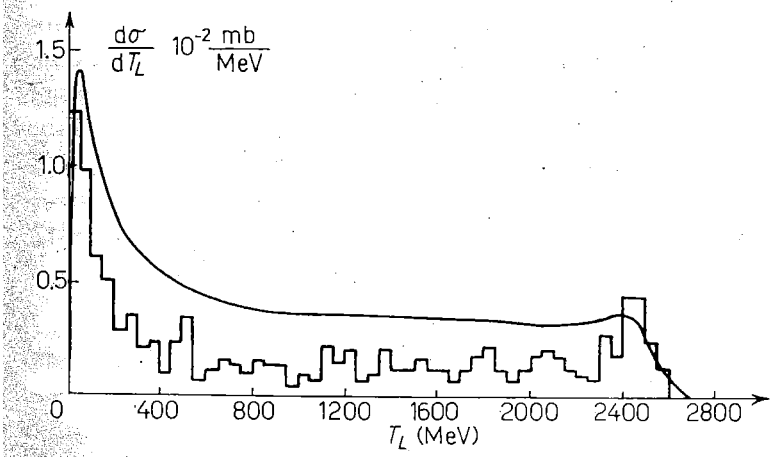


Fig. 5. – Theoretical and experimental spectrum of outgoing protons in the lab. system for the reaction $p+p \to p+p+\pi^0$ at 2.85 GeV of kinetic energy in the lab. system of the incoming protons.

broadening is so large that the peak disappears, but in any case we have a concentration of events at high energy.

Similar considerations hold also for reaction (2): in this case, further complications arise from the fact that all the 4 diagrams have the same weight and that in all of them $d$ and $f$ waves are present. The qualitative features discussed above can be, however, easily extended also to this case.

* * *

We thank Professor L. VAN HOVE for kind hospitality in the theoretical group at CERN, where an important part of this work has been carried out. We thank also the CERN Ferranti computer staff for invaluable help in the numerical calculations. We thank Drs. E. FERRARI and F. SELLERI for very useful suggestions and for continuous advice. We are indebted also to Professors M. CINI and R. GATTO for their interest in this work.

---

## RIASSUNTO

La produzione singola di pioni nell'urto nucleone-nucleone è calcolata nell'approssimazione di un solo pione scambiato. Sono stati calcolati tutti i possibili diagrammi di questo tipo nella « pole approximation » discussa nel testo; si è tenuto conto anche dei termini di interferenza fra essi. Sono stati calcolati gli spettri nell'energia nel laboratorio dei nucleoni finali e sono stati confrontati con i dati sperimentali a 2.85 GeV. Questo confronto mostra un notevole buon accordo per piccoli valori del quadrato del quadri-impulso del pione virtuale. Per valori più alti il comportamento qualitativo è ancora riprodotto, ma i valori teorici sono più grandi di quelli sperimentali.

3834